Application of a Coupled-Integral-Equations Technique to Ridged Waveguides

Smain Amari, Jens Bornemann, *Senior Member, IEEE,* and Ruediger Vahldieck, *Senior Member, IEEE*

***Abstract*— Cut-off frequencies of all TE and TM modes of a ridged rectangular wave guide are accurately determined using a coupled-integral equations technique (CIET). The technique analyzes both symmetric and asymmetric situations in one step. Basis functions, which include the edge conditions and mirror images in the waveguide walls, are used in the moment method solution of the integral equations. One or two basis functions are found sufficient to accurately determine the spectrum. The limiting case of a zero-thickness metallic ridge is also presented. Results from the present technique are compared with available data; excellent agreement is documented.**

I. Introduction

RIDGED WAVEGUIDES have been used in many microwave communication systems because of their extended bandwidth [1]–[2]. The first analysis of rectangular ridged waveguides was presented by Cohn using the transverse resonance method [3]. Using the same technique, Hopfer [4] and Pyle [5] presented improved results for the TE_{m0}. The cutoff frequencies were determined from a characteristic equation, which is derived from the transverse resonance condition, where the ridge is represented by its equivalent susceptance. The accuracy of the solution is, therefore, contingent on the availability of closed form and accurate expressions for the susceptance. Montgomery [6] computed the entire TE and TM spectrum of a ridge waveguide from an integral equation that was solved using the Ritz-Galerkin method. Utsumi [7] used a variational formulation, along with a trial function that satisfies the edge condition, to determine the spectrum of the structure and its modal field distributions. Omar and Schünemann [8] applied the generalized spectral domain technique to the symmetric ridge waveguide, where the axial components of the electromagnetic field are expanded in a series of basis functions which satisfy the edge conditions [8]. By expanding the axial components, however, basis functions covering the entire boundary of the ridge are required.

In all these reports, the analysis is limited to symmetric cases where electric or magnetic walls are assumed at the location of the plane of physical symmetry. The determination of the spectrum of the structure is carried out separately for each symmetry.

In the technique presented here, the TE spectrum is determined in one step regardless of the symmetry of the structure. Both symmetric and asymmetric ridges are handled through a single formulation and in a single step. The inclusion of information about the edge conditions and mirror images at each of the two metallic edges of the ridge allows accurate analysis of the spectrum of the system. An expansion of the tangential electric field, as presented in this paper, limits the support of the basis functions to a single interface and, therefore, results in a reduction in the size of the matrices involved in the moment method. The necessity of accurately determining the spectrum of asymmetric ridges is of prime importance for devices where the symmetry is broken and different polarizations are coupled. This paper presents an efficient and accurate method of analysis that achieves such a goal.

For an asymmetric ridge waveguide, we derive two coupled-integral equations for the tangential components of the electric field. These coupled integral equations are then solved using the method of moments. A major advantage of the coupled-integral equations technique (CIET) resides in the fact that it allows us to concentrate on those quantities that are not well behaved, namely the singular components of the electromagnetic field, and include that information in the basis functions. In addition, should the structure contain several points where the fields are singular, the CIET also readily includes that information.

The CIET takes into account all modes of the subregions into which the structure is divided. By doing so, it eliminates the phenomenon of relative convergence as all the inner products are accurately computed and tested for convergence. In other words, only one parameter is left in the numerical solution: the number of basis functions M. It will be seen that, even when trigonometric functions are used as basis functions, the cutoff wavenumbers are accurately determined with three or four basis functions while a single basis function, which includes the edge conditions, achieves similar, if not better, accuracy.

In the case of an infinitely thin metallic ridge, the entire spectrum is obtained from one integral equation for the TE and one for the TM modes. Basis functions that include the Maxwellian edge conditions are used in the numerical solution, resulting in a reduction in CPU time and increased accuracy. The results for the infinitely thin case can be used as starting values in the numerical solution of the coupled-integral equations when the ridge is of finite thickness, but not electrically thin.

The next section presents the derivation of the coupled integral equations for the tangential electric field.

Manuscript received March 8, 1996; revised August 26, 1996.

The authors are with the Laboratory for Lightwave Electronics, Microwaves and Communications, LLiMiC, Department of Electrical and Computer Engineering, University of Victoria, Victoria B.C., V8W 3P6 Canada.

Publisher Item Identifier S 0018-9480(96)08508-0.

II. Transverse Electric Modes

We consider the structure shown in Fig. 1. It consists of a metallic ridge of width $2s$ and height $b-d$, which is placed at a distance l_1 from the left wall of a rectangular waveguide of cross section $2a \times b$. All metallic surfaces are assumed lossless in this analysis. No assumption about the symmetry of the structure or the dimensions of the ridge is made.

It is obvious that the dominant physics of the problem takes place in the vicinity of the metallic ridge, especially at the sharp corners where the transverse components of the electromagnetic fields are singular [9]. To guarantee numerical efficiency, the formulation should capture this singular behavior from the outset. An integral formulation of the tangential electric field at the interfaces I-II and II-III provides such a mechanism (Fig. 1). The TE modes are considered first.

The transverse components of a TE mode are determined from the axial component of the magnetic field, H_z. It is also important to note that, at cutoff, the transverse components of the magnetic field, H_x and H_y, are both identically zero. It is, therefore, sufficient to enforce the continuity conditions for the remaining tangential components, namely H_z and E_y.

Following the mode-matching technique (MMT), we expanded H_z and E_y in modal expansions of the following forms:

$$H_z^I(x,y) = \sum_{n=0}^{\infty} A_n^I \frac{\cosh(\gamma_{1n}x)}{\cosh(\gamma_{1n}l_1)} \cos\left[\frac{n\pi}{b}y\right] \tag{1.a}$$

$$H_z^{II}(x,y) = \sum_{n=0}^{\infty} [A_n^{II} e^{\gamma_{2n}x} + B_n^{II} e^{-\gamma_{2n}x}] \cos\left[\frac{n\pi}{d}y\right] \tag{1.b}$$

$$H_z^{III}(x,y) = \sum_{n=0}^{\infty} A_n^{III} \frac{\cosh(\gamma_{1n}(x-2a))}{\cosh(\gamma_{1n}l_2)} \cos\left[\frac{n\pi}{b}y\right] \tag{1.c}$$

and

$$E_y^I(x,y) = \sum_{n=0}^{\infty} A_n^I \gamma_{1n} \frac{\sinh[\gamma_{1n}x]}{\sinh[\gamma_{1n}l_1]} \cos\left[\frac{n\pi}{b}y\right] \tag{2.a}$$

$$E_y^{II}(x,y) = \sum_{n=0}^{\infty} \gamma_{2n}[A_n^{II} e^{\gamma_{2n}x} - B_n^{II} e^{-\gamma_{2n}x}] \cos\left[\frac{n\pi}{d}y\right] \tag{2.b}$$

$$E_y^{III}(x,y) = \sum_{n=0}^{\infty} \gamma_{1n} A_n^{III} \frac{\sinh(\gamma_{1n}(x-2a))}{\cosh(\gamma_{1n}l_2)} \cos\left[\frac{n\pi}{b}y\right]. \tag{2.c}$$

In these equations, $\gamma_{1n}^2 = (n\pi/b)^2 - k_c^2$ and $\gamma_{2n}^2 = (n\pi/d)^2 - k_c^2$, where k_c is the cutoff wavenumber.

The boundary conditions of the problem are

$$E_y^I(x = l_1, y) = 0, \qquad d \le y \le b \tag{3.a}$$

$$E_y^{II}(x = l_1, y) = E_y^{II}(x = l_1, y), \qquad 0 \le y \le d \tag{3.b}$$

$$E_y^{II}(x = l_1 + 2s, y) = E_y^{III}(x = l_1 + 2s, y), \qquad 0 \le y \le d \tag{3.c}$$

$$E_y^{III}(x = l_1 + 2s, y) = 0, \qquad d \le y \le b \tag{3.d}$$

$$H_z^I(x = l_1, y) = H_z^{II}(x = l_1, y), \qquad d \le y \le b \tag{4.a}$$

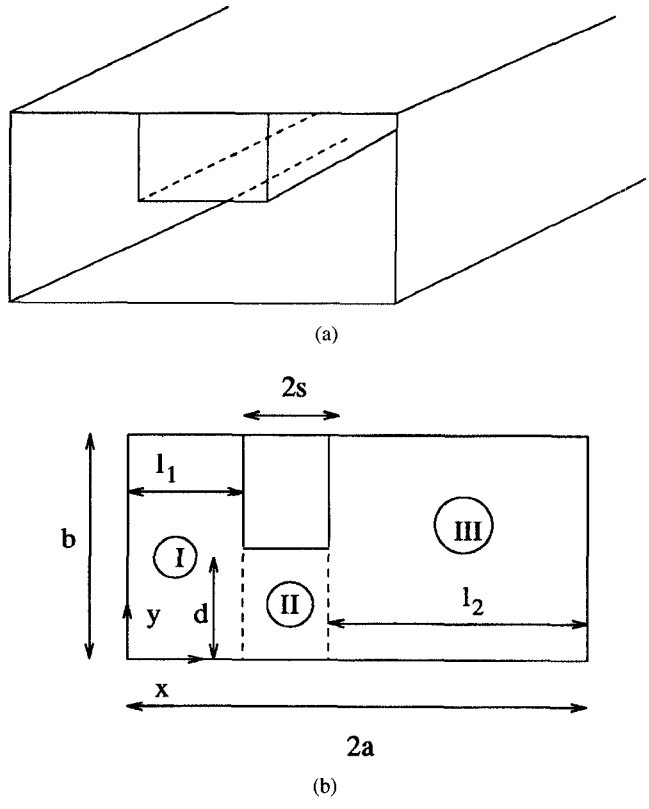

Fig. 1. Geometry of a rectangular ridge waveguide and coordinate system.

and

$$H_z^{II}(x = l_1 + 2s, y) = H_z^{III}(x = l_1 + 2s, y), \qquad d \le y \le b. \tag{4.b}$$

Instead of following the MMT, we rewrite the boundary conditions of the tangential electric field, (3), in a different form. Let the true distribution of the tangential electric field E_y at the two interfaces be denoted by $f_1(y)$ and $f_2(y)$, respectively. It is then easy to verify that (3) can be cast in the form

$$E_y^I(x = l_1, y) = f_1(y)$$
$$E_y^{II}(x = l_1, y) = f_1(y) \tag{5.a}$$

and

$$E_y^{II}(x = l_1 + 2s, y) = f_2(y)$$
$$E_y^{III}(x = l_1 + 2s, y) = f_2(y) \tag{5.b}$$

as long as the functions $f_1(y)$ and $f_2(y)$ satisfy the following condition:

$$f_1(y) = f_2(y) = 0, \qquad d \le y \le b. \tag{6}$$

The introduction of the functions f_1 and f_2 allows us to include in the formulation whatever information we have about the tangential electric field at the interface, in particular its singular nature.

Equations (5.a) and (5.b) are now used in the modal expansions given by (2) to project out the modal expansion

coefficients leading to

$$A_n^I = \frac{\tilde{f}_1^I(n)}{\gamma_{1n}\tanh(\gamma_{1n}l_1)} \tag{7.a}$$

$$A_n^{II} = e^{-\gamma_{2n}l_1}\frac{\tilde{f}_2^{II}(n) - \tilde{f}_1^{II}(n)e^{-2\gamma_{2n}s}}{2\gamma_{2n}\sinh[2\gamma_{2n}s]} \tag{7.b}$$

$$B_n^{II} = e^{\gamma_{2n}l_1}\frac{\tilde{f}_2^{II}(n) - \tilde{f}_1^{II}(n)e^{2\gamma_{2n}s}}{2\gamma_{2n}\sinh[2\gamma_{2n}s]} \tag{7.c}$$

and

$$A_n^{III} = -\frac{\tilde{f}_2^I(n)}{\gamma_{1n}\tanh(\gamma_{1n}l_2)}. \tag{7.d}$$

The following notations were introduced for convenience

$$\tilde{f}^I(n) = \frac{2/b}{1+\delta_{n0}}\int_0^d f(y)\cos\left[\frac{n\pi}{b}y\right]dy \tag{8.a}$$

and

$$\tilde{f}^{II}(n) = \frac{2/d}{1+\delta_{n0}}\int_0^d f(y)\cos\left[\frac{n\pi}{d}y\right]dy. \tag{8.b}$$

The functions f_1 and f_2 are determined from the boundary conditions of the tangential magnetic field, i.e, (4), which we rewrite in the form

$$\sum_{n=0}^{\infty}\frac{\tilde{f}_1^I(n)}{\gamma_{1n}\tanh[\gamma_{1n}l_1]}\cos\left[\frac{n\pi}{b}y\right] + \left[\frac{\tilde{f}_1^{II}(n)}{\gamma_{2n}\tanh[2\gamma_{2n}s]} - \frac{\tilde{f}_1^{II}(n)}{\gamma_{2n}\sinh[2\gamma_{2n}s]}\right]\cdot\cos\left[\frac{n\pi}{d}y\right] = 0 \tag{9}$$

and

$$\sum_{n=0}^{\infty}\frac{\tilde{f}_1^I(n)}{\gamma_{1n}\tanh[\gamma_{1n}l_1]}\cos\left[\frac{n\pi}{b}y\right] + \left[\frac{\tilde{f}_1^{II}(n)}{\gamma_{2n}\tanh[2\gamma_{2n}s]} - \frac{\tilde{f}_1^{II}(n)}{\gamma_{2n}\sinh[2\gamma_{2n}s]}\right]\cdot\cos\left[\frac{n\pi}{d}y\right] = 0. \tag{10}$$

It is important to emphasize that (9) and (10) hold only in the interval $0 \le y \le d$. These two coupled-integral equations in the functions f_1 and f_2 fully describe the TE spectrum of the system.

To transform these integral equations into matrix forms, we expand the unknown functions in a series of basis functions $B_i(y)$. Since the tangential electric field has the same analytic structure at the two interfaces, the same basis functions are used for both f_1 and f_2. We can therefore write

$$f_1(y) = \sum_{i=1}^{M} c_i B_i(y) \tag{11.a}$$

and

$$f_2(y) = \sum_{i=1}^{N} d_i B_i(y). \tag{11.b}$$

The number of terms, N and M in these expansions, are increased until convergence is achieved. For ease of implementation, we take $M = N$ in this work; it will be seen that $N = M = 1$ is sufficient.

Let also $T_k(x), k = 1, 2, \cdots$ denote a testing function for the tangential magnetic field at the interface. Substituting (11) in (9) and (10), multiplying by $T_k(y)$, and integrating we get two sets of linear equations in the expansion coefficients c and d, namely

$$\begin{aligned}[U][c] + [V][d] &= 0\\ [V][c] + [W][d] &= 0\end{aligned} \tag{12}$$

where

$$[U]_{ij} = \sum_{n=0}^{\infty}(1+\delta_{n0})\left[\frac{\tilde{B}_j^I(n)\tilde{T}_i^I(n)}{\gamma_{1n}\tanh[\gamma_{1n}l_1]} + \frac{d}{b}\frac{\tilde{B}_j^{II}(n)\tilde{T}_i^{II}(n)}{\gamma_{2n}\tanh[2\gamma_{2n}s]}\right], \qquad i,j = 1,\cdots,M \tag{13.a}$$

$$[V]_{ij} = -\frac{d}{b}\sum_{n=0}^{\infty}\frac{(1+\delta_{n0})\tilde{T}_i^{II}(n)\tilde{B}_j^{II}(n)}{\gamma_{2n}\sinh[2\gamma_{2n}s]} \tag{13.b}$$

and

$$[U]_{ij} = \sum_{n=0}^{\infty}(1+\delta_{n0})\left[\frac{\tilde{B}_j^I(n)\tilde{T}_i^I(n)}{\gamma_{1n}\tanh[\gamma_{1n}l_2]} + \frac{d}{b}\frac{\tilde{B}_j^{II}(n)\tilde{T}_i^{II}(n)}{\gamma_{2n}\tanh[2\gamma_{2n}s]}\right], \qquad i,j = 1,\cdots,M. \tag{13.c}$$

The cutoff frequencies of the TE modes are determined as the zeros of the determinant of the matrix in (12). It is numerically more advantageous to locate the zero of the smallest singular value instead, as this allows the suppression of the poles that are otherwise present in the determinant [10].

When the thickness of the ridge is electrically small it is convenient to have the results for the infinitely thin metallic ridge as starting guess. The integral equation giving the tangential electric field $f(y)$ at the interface can be derived following the same steps as above. If the infinitely thin metallic ridge is located at $x = l_1$, this equation is written as

$$\sum_{n=0}^{\infty}\left[\frac{\tilde{f}^I(n)}{\gamma_{1n}\tanh[\gamma_{1n}l_1]} + \frac{\tilde{f}^I(n)}{\gamma_{1n}\tanh[\gamma_{1n}l_2]}\right]\cos\left[\frac{n\pi}{b}y\right], \qquad 0 \le y \le d. \tag{14}$$

The function $f(y)$, which satisfies (6), is expanded in a series of basis functions that include the edge conditions of an infinitely thin conductor. The expansion coefficients are determined using the moment method as in the previous case.

III. Basis and Testing Functions for TE Modes

Two salient features should be included in the basis functions to accelerate convergence: 1) the edge conditions at $(x, y) = (l_1, d)$ and $(x, y) = (l_1 + 2s, d)$ (see Fig. 1); and 2) their Fourier spectrum in each of the subregions should not be a numerical burden itself.

Recall that at a 90° metallic edge, the components of the electric field, which are transverse to the axis of the wedge, are singular as $r^{-1/3}$, where r is the radial distance from the edge.

On the other hand, at a 180° edge, the normal component of the electric field behaves as r^0 [9]. It is also possible to include in the basis functions the fact that there is an electric wall at $y = 0$. In other words, the edge conditions should also be mirrored into this wall. A set of basis functions that satisfy all these criteria are given by

$$B_i(y) = \frac{\cos\left[(i-1)\pi\frac{y}{d}\right]}{\left(1-\left(\frac{y}{d}\right)^2\right)^{1/3}}, \qquad i = 1, 2, \cdots. \tag{15}$$

The Fourier spectrum of these basis functions, i.e, the quantities $\tilde{B}_i^I(n)$ and $\tilde{B}_i^{II}(n)$, are expressible in terms of Bessel functions of the first kind of order 1/6, $J_{1/6}$ [11]. More specifically

$$\tilde{B}_i^I(n) = \frac{d/b}{1+\delta_{n0}}\frac{1}{2}\Gamma(1/2)\Gamma(2/3)\left[\frac{J_{1/6}((i-1+nd/b)\pi)}{((nd/b+i-1)\pi/2)^{1/6}} + \frac{J_{1/6}(|i-1-nd/b|\pi)}{(|nd/b-i+1|\pi/2)^{1/6}}\right] \tag{16.a}$$

and

$$\tilde{B}_i^{II}(n) = \frac{1}{1+\delta_{n0}}\frac{1}{2}\Gamma(1/2)\Gamma(2/3)\left[\frac{J_{1/6}((i-1+n)\pi)}{((i-1+n)\pi/2)^{1/6}} + \frac{J_{1/6}(|i-1-n|\pi)}{(|i-1-n|\pi/2)^{1/6}}\right] \tag{16.b}$$

where Γ is the Gamma function. When the argument of one of the Bessel functions vanishes, the corresponding term should be replaced by the quantity

$$Q_i(n) = \frac{1}{1+\delta_{n0}}\frac{1}{2}\frac{\Gamma(1/2)\Gamma(2/3)}{\Gamma(7/6)}, \qquad i-1 = n. \tag{17}$$

Although the spectrum of the basis functions in each of the subregions involves Bessel functions, most of the arguments in these functions are large. Asymptotic expansions can be fruitfully used with very little loss in accuracy. It is also true that most of these spectra are localized around the zero value of their argument. Hence, the sums in (13) are dominated by only a few terms.

The testing functions are used in projecting the tangential magnetic field in the interval $0 \le y \le d$. To extract as much information about this quantity with only a few projections, it is important to be able to include in the testing functions the qualitative features of $H_z(y)$. The edge conditions correspond to a nonanalytic behavior of the form $r^{1/3}$ at the 90° edge and the fact that it approaches a constant at $y = 0$, i.e., behaves as r^0. Taking into account the presence of the electric wall at $y = 0$, the following testing functions are used in this work:

$$T_i(y) = \frac{\cos\left[(i-1/2)\pi\frac{y}{d}\right]}{\left(1-\left(\frac{y}{d}\right)^2\right)^{1/3}}, \qquad i = 1, 2, \cdots. \tag{18}$$

The Fourier spectra of these functions can also be expressed in terms of Bessel functions of order 1/6 [11]

$$\tilde{T}_i^I(n) = \frac{d/b}{1+\delta_{n0}}\frac{1}{2}\Gamma(1/2)\Gamma(2/3) \cdot \left[\frac{J_{1/6}((i-1/2+nd/b)\pi)}{((nd/b+i-1/2)\pi/2)^{1/6}} + \frac{J_{1/6}(|i-1/2-nd/b|\pi)}{(|nd/b-i+1/2|\pi/2)^{1/6}}\right] \tag{19.a}$$

and

$$\tilde{T}_i^{II}(n) = \frac{1}{1+\delta_{n0}}\frac{1}{2}\Gamma(1/2)\Gamma(2/3)\left[\frac{J_{1/6}((i-1/2+n)\pi)}{((i-1/2+n)\pi/2)^{1/6}} + \frac{J_{1/6}(|i-1/2-n|\pi)}{(|i-1/2-n|\pi/2)^{1/6}}\right]. \tag{19.b}$$

When the argument of the Bessel function vanishes the corresponding term should be replaced by the expression given in (16).

The limiting case of an infinitely thin ridge presents a Maxwellain singularity at the tip of the ride. A set of basis functions for this case is given by

$$Z_i(y) = \frac{\cos\left[(i-1)\pi\frac{y}{d}\right]}{\sqrt{1-\left(\frac{y}{d}\right)^2}}, \qquad i = 1, 2, \cdots. \tag{20}$$

The Fourier spectra of these basis functions are given by

$$\tilde{Z}_i^I(n) = \frac{\pi/2}{1+\delta_{n0}}[J_0[\pi(i-1+nd/b)] + J_0(\pi|i-1-nd/b|)]. \tag{21}$$

IV. Transverse Magnetic Modes

Transverse magnetic modes have a nonvanishing component of the axial electric field, E_z, from which the remaining components can be obtained.

Note also that, at cutoff, the transverse components of the electric field are all zero; we need to focus only on the component of the magnetic field which is tangential to the interfaces, i.e., on H_y.

In each of the regions I, II, and III, E_z is expanded in modes that satisfy all the boundary conditions of the region except those in the planes of the interfaces

$$E_z^I(x,y) = \sum_{n=1}^{\infty} A_n^I \frac{\sinh[\gamma_{1n}x]}{\sinh[\gamma_{1n}l_1]}\sin\left[n\pi\frac{y}{b}\right] \tag{22.a}$$

$$E_z^{II}(x,y) = \sum_{n=1}^{\infty}[A_n^{II}e^{\gamma_{2n}x} + B_n^{II}e^{-\gamma_{2n}x}]\sin\left[\frac{n\pi}{d}y\right] \tag{22.b}$$

$$E_z^{III}(x,y) = \sum_{n=1}^{\infty} A_n^{III}\frac{\sinh[\gamma_{1n}(x-2a)]}{\sinh[\gamma_{1n}l_2]}\sin\left[n\pi\frac{y}{b}\right] \tag{22.c}$$

$$H_y^I(x,y) = \frac{-1}{j\omega\mu_0}\sum_{n=1}^{\infty} A_n^I\gamma_{1n}\frac{\cosh[\gamma_{1n}x]}{\sinh[\gamma_{1n}l_1]}\sin\left[n\pi\frac{y}{b}\right] \tag{23.a}$$

$$H_y^{II}(x,y) = \frac{-1}{j\omega\mu_0}\sum_{n=1}^{\infty}\gamma_{2n}[A_n^{II}e^{\gamma_{2n}x} - B_n^{II}e^{-\gamma_{2n}x}] \cdot \sin\left[\frac{n\pi}{d}y\right] \tag{23.b}$$

and

$$H_y^{III}(x,y) = \frac{-1}{j\omega\mu_0}\sum_{n=1}^{\infty}A_n^{III}\gamma_{1n}\frac{\sinh[\gamma_{1n}(x-2a)]}{\sinh[\gamma_{1n}l_2]} \cdot \sin\left[n\pi\frac{y}{b}\right]. \tag{23.c}$$

The boundary conditions of these modes are

$$E_z^I(x=l_1,y) = E_z^{III}(x=l_1+2s,y) = 0, \quad d \le y \le a \tag{24.a}$$

$$E_z^I(x=l_1,y) = E_z^{II}(xl_1,y), \quad 0 < y \le d \tag{24.b}$$

$$E_z^{II}(x=l_1+2s,y) = E_z^{III}(x=l_1+2s,y), \quad 0 < y \le d \tag{24.c}$$

$$H_y^I(x=l_1,y) = H_y^{II}(xl_1,y), \quad 0 < y \le d \tag{24.d}$$

and

$$H_y^{II}(x=l_1+2s,y) = H_y^{III}(x=l_1+2s,y), \quad 0 < y \le d. \tag{24.e}$$

Following similar steps to those for the analysis of the TE modes, we introduce two functions $g_1(y)$ and $g_2(y)$, which represent the quantity E_z at the two interfaces, respectively, and rewrite the boundary conditions (24) as

$$E_z^I(x=l_1,y) = g_1(y)$$
$$E_z^{II}(x=l_1,y) = g_1(y) \tag{25.a}$$

and

$$E_z^{II}(x=l_1+2s,y) = g_2(y)$$
$$E_z^{III}(x=l_1+2s,y) = g_2(y). \tag{25.b}$$

The forms given by (25) guarantee that the boundary conditions of the electric field are *always* satisfied as long as the functions g_1 and g_2 satisfy (6).

The coupled integral equations, which govern g_1 and g_2, are derived from combining the expansions given in (23) with (25) and the boundary conditions (24). The algebra is straightforward and leads to

$$\sum_{n=1}^{\infty}\left\{\frac{\tilde{g}_1^I(n)\gamma_{1n}}{\tanh[\gamma_{1n}l_1]}\sin\left[n\pi\frac{y}{b}\right] + \left[\frac{\tilde{g}_1^{II}(n)\gamma_{2n}}{\tanh[\gamma_{2n}l_1]} - \frac{\tilde{g}_2^{II}\gamma_{2n}}{\sinh[2\gamma_{2n}s]}\right]\sin\left[n\pi\frac{y}{d}\right]\right\} = 0 \tag{26}$$

and

$$\sum_{n=1}^{\infty}\left\{\frac{\tilde{g}_2^I(n)\gamma_{1n}}{\tanh[\gamma_{1n}l_2]}\sin\left[n\pi\frac{y}{b}\right] + \left[\frac{\tilde{g}_2^{II}(n)\gamma_{2n}}{\tanh[\gamma_{2n}l_1]} - \frac{\tilde{g}_1^{II}\gamma_{2n}}{\sinh[2\gamma_{2n}s]}\right]\sin\left[n\pi\frac{y}{d}\right]\right\} = 0. \tag{27}$$

For the TM modes, the following notation is used:

$$\tilde{g}^I(n) = \frac{2}{b}\int_0^d g(y)\sin\left[n\pi\frac{y}{b}\right]dy \tag{28.a}$$

and

$$\tilde{g}^{II}(n) = \frac{2}{d}\int_0^d g(y)\sin\left[n\pi\frac{y}{d}\right]dy. \tag{28.b}$$

To solve these two coupled-integral equations, we expand the functions $g_1(y)$ and $g_2(y)$ using a set of basis functions as in the TE case. Obviously, the basis functions for the TE and TM modes are different. If $H_i(y)$ denotes a generic basis function for the TM modes, we write g_1 and g_2 as

$$g_1(y) = \sum_{i=1}^{N}p_iH_i(y)$$
$$g_2(y) = \sum_{i=1}^{N}q_iH_i(y). \tag{29}$$

If testing functions $L_i(y)$ are used to sample the magnetic field boundary condition given by (26) and (27), the expansion coefficients p_i and q_i are found to satisfy the following homogeneous coupled sets:

$$[X][p] + [Y][q] = 0$$
$$[Y][p] + [Z][q] = 0 \tag{30}$$

where

$$[X]_{ij} = \sum_{n=0}^{\infty}\left[\frac{\tilde{H}_j^I(n)\tilde{L}_i^I(n)\gamma_{1n}}{\tanh[\gamma_{1n}l_1]} + \frac{d}{b}\frac{\tilde{H}_j^{II}(n)\tilde{L}_i^{II}(n)\gamma_{2n}}{\tanh[2\gamma_{2n}s]}\right], \quad i,j = 1,\cdots,M \tag{31.a}$$

$$[Y]_{ij} = -\frac{d}{b}\sum_{n=0}^{\infty}\frac{\tilde{L}_i^{II}(n)\tilde{H}_j^{II}(n)\gamma_{2n}}{\sinh[2\gamma_{2n}s]} \tag{31.b}$$

and

$$[Z]_{ij} = \sum_{n=0}^{\infty}\left[\frac{\tilde{H}_j^I(n)\tilde{L}_i^I(n)\gamma_{1n}}{\tanh[\gamma_{1n}l_2]} + \frac{d}{b}\frac{\tilde{H}_j^{II}(n)\tilde{L}_i^{II}(n)\gamma_{2n}}{\tanh[2\gamma_{2n}s]}\right], \quad i,j = 1,\cdots,M. \tag{31.c}$$

The cutoff frequencies of the TM modes are given by the zeros of the determinant of the coupled linear systems in (30). To avoid the poles in the determinant, the zero of the smallest singular value of the system is located instead [10].

The TM modes of an infinitely thin metallic ridge of height $b-d$ and located at $x = l_1$ are analyzed in analogy with the TE modes. The function $g(y)$, which represents the tangential electric field E_z at the interface, satisfies the following integral equation:

$$\sum_{n=1}^{\infty}\frac{\tilde{g}^I(n)\gamma_{1n}}{\tanh[\gamma_{1n}l_1]} + \frac{\tilde{g}^I(n)\gamma_{1n}}{\tanh[\gamma_{1n}l_2]}\sin\left[n\pi\frac{y}{b}\right] = 0, \quad 0 \le y \le d. \tag{32}$$

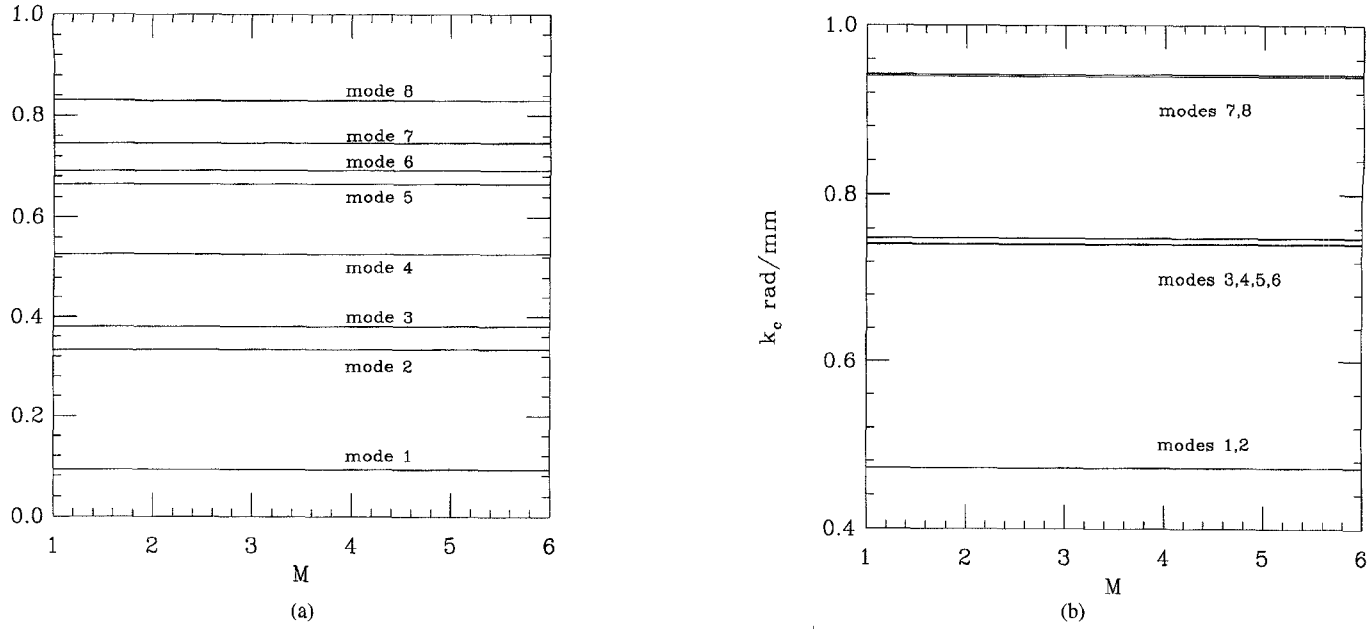

Fig. 2. Convergence of the cutoff wavenumbers of the first eight-mode s when edge-conditioned basis functions are used. $a = b9.5$ mm, $d = 1.7$ mm, $s = 0.15$ mm. (a) TE modes. (b) TM modes.

By expanding the function $g(y)$ in an appropriate set of basis functions, this integral equation is solved by the standard moment method.

V. Basis Functions for TM Modes

The basis functions that are used to expand the tangential electric field E_z at the interface should each include the edge conditions at $(x, y) = (l_1, d)$ and $(x, y) = (l_1 + 2s, d)$. In the vicinity of $(x, y) = (l_1, d)$ and $(x, y) = (l_1 + 2s, d)$, E_z vanishes as $r^{2/3}$ and as r^1 as $y \to 0$ [9]. Taking account of the fact that an electric wall exists at $y = 0$, it can easily be verified that the following basis functions satisfy these conditions.

$$G_i(x) = \frac{\sin\left[i\pi\frac{y}{d}\right]}{\left[\left(1-\left(\frac{y}{d}\right)^2\right]^{1/3}}, \qquad i = 1, 2, \cdots. \tag{33}$$

The spectra of these functions over the modes of regions I and II can be expressed in terms of Bessel functions of the first kind of order 1/6, $J_{1/6}$ [11]

$$\tilde{G}_i^I(n) = \frac{d}{b}\frac{1}{2}\Gamma(1/2)\Gamma(2/3)\left[\frac{J_{1/6}(|i-nd/b|\pi)}{(|i-nd/b|\pi/2)^{1/6}} - \frac{J_{1/6}((i+nd/b)\pi)}{((i+nd/b)\pi/2)^{1/6}}\right] \tag{34.a}$$

and

$$\tilde{G}_i^{II}(n) = \frac{1}{2}\Gamma(1/2)\Gamma(2/3)\left[\frac{J_{1/6}[|i-n|\pi]}{[|i-n|\pi/2]^{1/6}} - \frac{J_{1/6}[(i+n)\pi]}{[(i+n)\pi/2]^{1/6}}\right]. \tag{34.b}$$

For the TM modes the testing functions are taken equal to the basis functions $L_i(y) = G_i(y)$.

The basis functions for the infinitely thin metallic ridge should include the nonanalytic behavior of E_z. Taking into account the mirror image in the electric wall at $y = 0$, the following basis functions are used:

$$G_i^0(y) = \frac{\sin\left[i\pi\frac{y}{d}\right]}{\sqrt{\left(1-\left(\frac{y}{d}\right)^2\right.}}, \qquad i = 1, 2. \tag{35}$$

The spectra of these basis functions are given in terms of the Bessel function J_0

$$\tilde{G}_i^{0I}(n) = \frac{\pi}{2}\{J_0[\pi|i-nd/b|] - J_0[\pi(i+nd/b)]\}. \tag{36}$$

VI. Numerical Results and Discussion

The CIET is used to compute the spectrum of the ridge rectangular waveguide shown in Fig. 1. To validate the theory and the computer code, we compare results from the present work to those given in [4], [7], and [8] for the symmetric ridge ($l_1 = l_2 = a$).

Fig. 2 shows the cutoff wavenumbers in rad/mm of the first eight TE modes when upto six basis functions, which include the edge condition and the mirror imaging in the waveguide walls, are used. The results clearly demonstrate that one or two basis functions are sufficient; consequently, only two basis functions are used in the following calculations.

Table I shows the cutoff wavenumbers of the first eight TE modes in rad/mm when $a = b = 9.5$ mm, $s = 0.15$ mm, and $d = 1.7$ mm. The agreement with data from [7] and [8] is excellent as it can be clearly seen. The same table also

TABLE I
CUTOFF WAVENUMBERS (rad/mm) OF THE FIRST EIGHT TE MODES IN A SINGLE-RIDGE WAVEGUIDE

Mode	1	2	3	4	5	6	7	8
Present Method	0.0926	0.3332	0.3811	0.5263	0.6653	0.6916	0.7453	0.8295
Ref.[7]	0.0930	0.3332	0.3881	0.5265	0.6654	0.6913	0.7456	0.8298
Ref.[8]	0.0928	0.3332	0.3810	0.5262	0.6654	0.6912	0.7456	0.8294
s=0-approx.	0.0968	0.3309	0.3811	0.5284	0.6621	0.6853	0.7411	0.8316

a = b = 9.5 mm, s = 0.15 mm, d = 1.7 mm

TABLE II
CUTOFF WAVENUMBERS (rad/mm) OF THE FIRST EIGHT TE MODES IN A SINGLE-RIDGE WAVEGUIDE WHEN TRIGONOMETRIC FUNCTIONS ARE USED AS BASIS FUNCTIONS

M Mode	1	2	3	4	5	6	7	8
1	0.0910	0.3330	0.3800	0.5245	0.6653	0.6910	0.7453	0.8280
2	0.0925	0.3337	0.3811	0.5263	0.6653	0.6910	0.7453	0.8295
3	0.0928	0.3332	0.3810	0.5262	0.6654	0.6912	0.7455	0.8294
4	0.0928	0.3332	0.3810	0.5263	0.6654	0.6912	0.7455	0.8294
5	0.0928	0.3332	0.3810	0.5263	0.6654	0.6912	0.7455	0.8294
6	0.0928	0.3332	0.3810	0.5263	0.6654	0.6912	0.7455	0.8294
20	0.0928	0.3330	0.3810	0.5263	0.6654	0.6912	0.7455	0.8294

a = b = 9.5 mm, s = 0.15 mm, d = 1.7 mm

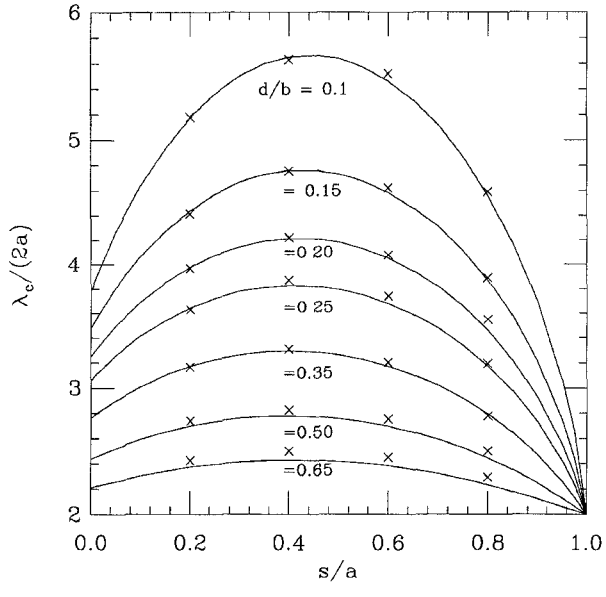

Fig. 3. Cutoff wavelengths $\lambda_c/(2a)$ as a function of s/a for different values of d/b. Two basis functions were used in obtaining these results. The crosses are from [4] and $b = 0.45a$.

gives the corresponding cutoff frequencies of the infinitely thin metallic ridge. Except for the first mode, where the relative error is of the order of 4%, the differences between the cutoff frequencies obtained from the infinitely thin assumption and those of the ridge of thickness $2s = 0.3$ mm are minor. When the thickness of the ridge is small compared to the dimensions of the waveguide, the results of the zero-thickness approximation can be used as starting values in the search for the cutoff wavenumbers of the actual structure.

The dependence of the cutoff wavelength of the fundamental mode TE_{10} on the thickness of the symmetric ridge is shown in Fig. 3 for different values of the ratio d/b when $b = 0.45a$. The crosses are from [4]. The agreement is good, except when $d/b = 0.65$, where an error of the order of 5% is found when $s/a = 0.8$.

To test the capability of the formulation to analyze asymmetric structures, the cutoff wavelength of the fundamental mode as a function of the location of the ridge was computed (Fig. 4). As expected, the largest effect takes place when the ridge is located at the maximum of the electric field of the unperturbed fundamental mode of the waveguide. The cutoff wavenumber obtained when $l_1/a = 1$ is identical to that given in Table I.

To test the sensitivity of the method to the nature of the basis functions, trigonometric functions were also used to compute the TE spectrum of a symmetric ridge. Table II shows the convergence of the cutoff wavenumbers as the number of basis functions is increased. It is clearly seen that the results obtained with three or more basis functions agree well with those given in [7] and [8]. It is worth emphasizing that the relevant inner products in (13) and (31) should be accurately computed by numerically testing for their convergence, thereby leaving only one parameter in the approximate solution, i.e, the number of basis functions. The standard mode-matching technique corresponds to truncating the sums at a fixed threshold. As the number of basis functions is increased, the truncated sums fail to accurately describe

TABLE III
CUTOFF WAVENUMBERS (rad/mm) OF THE FIRST EIGHT TM MODES IN A SINGLE-RIDGE WAVEGUIDE

Mode	1	2	3	4	5	6	7	8
Present Method	0.4711	0.4714	0.7410	0.7416	0.7481	0.7487	0.9400	0.9422
Ref.[4]	0.4665		0.7358					0.9427
s=0-approx.	0.4672		0.7371					0.9315

a = b = 9.5 mm, s = 0.15 mm, d = 1.7 mm

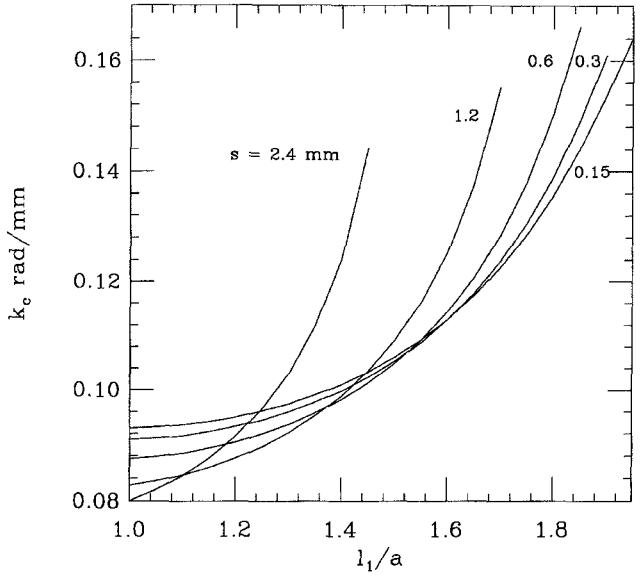

Fig. 4. Cutoff wavenumber of the fundamental mode as a function of the position of the ridge. $b = a = 9.5$ mm, $s = 0.15$ mm, and $d = 1.7$ mm.

the basis functions resulting in the phenomenon of relative convergence.

The cutoff wavelengths of the TM modes were also computed using the CIET. Table III shows the cutoff wavenumbers of the first eight TM modes along with those presented in [7]. It is interesting to note that the modes reported in [7] agree well with those of the infinitely thin approximation when $d = 1.7$ mm, $s = 0.15$ mm, and $b = a = 9.5$ mm. A close scrutiny of the behavior of the minimum singular value shows that there are, in fact, eight modes whose cutoff wavenumbers are smaller than 1 rad/mm. Only three of these were reported in [7]. Four of these cutoff wavenumbers are clustered around 0.74 rad/mm, two around 0.46 rad/mm, and two more around 0.93 rad/mm. For the infinitely thin and symmetric ridge, these three groups are degenerate as can be seen from a direct analysis with electric and magnetic walls at the position of the infinitely thin ridge.

VII. CONCLUSION

A CIET was presented and applied to determined the TE and TM spectrum of a ridge rectangular waveguide. The formulation allows the inclusion of the edge condition at more than one plane, thereby effectively handling asymmetric as well as symmetric structures. By testing the sums in the inner products for convergence, the phenomenon of relative convergence is not encountered. One or two basis functions, which include the edge condition and are mirror-imaged in the walls of the waveguide, are sufficient to determine the spectrum of the structure. Excellent agreement between the presented results and the literature is documented. The technique is readily applicable to more complicated situations where edge conditions are present at more than two locations.

REFERENCES

[1] P. A. Rizzi, *Microwave Engineering, Passive Circuits*. Englewood Cliffs, NJ: Prentice Hall, 1988.
[2] J. Uher, J. Bornemann, and U. Rosenberg, *Waveguide Components for Antenna Feed Systems: Theory and CAD*. Dedham, MA: Artech House, 1993.
[3] S. B. Cohn, "Properties of ridge waveguide," *Proc. IRE*, vol. 3 5, pp. 783–388, Aug. 1947.
[4] S. Hopfer, "The design of ridged waveguides," *IRE Trans. Microwave Theory Tech.*, pp. 20–29, Oct. 1955.
[5] J. R. Pyle, "The cutoff wavelength of the TE_{10} mode in ridged rectangular waveguide of any aspect ratio," *IEEE Trans. Microwave Theory Tech.*, vol. 14, pp. 175–183, Apr. 1966.
[6] J. P. Momtgomery, "On the complete eigenvalue solution of ridged waveguide," *IEEE Trans. Microwave Theory Tech.*, vol. 19, pp. 547–555, June 1971.
[7] Y. Utsumi, " Variational analysis of ridged waveguide modes," *IEEE Trans. Microwave Theory Tech.*, vol.. MTT-32, pp. 111–120, Feb. 1985.
[8] A. S. Omar and K. F. Schünemann, "Application of the general ized spectral-domain technique to the analysis of rectangular waveguides with rectangular and circular metallic inserts," *IEEE Trans. Microwave Theory Tech.*, vol. 39, pp. 944–952, June 1991.
[9] R. E. Collin, *Field Theory of Guided Waves*. New York: IEEE Press, 1991.
[10] V. Labay and J. Bornemann, "Matrix singular value decomposition for pole free solutions of homogeneous matrix equations as applied to numerical modeling," *IEEE Microwave Guided Wave Lett.*, vol. 2, pp. 49–51, Feb. 1992.
[11] I. S. Gradshteyn and I. M. Ryznik, *Tables of Integrals, Series, and Products*, 5th ed. New York: Academic, 1994.

Smain Amari received the DES degree in physics and electronics from Constantine University, Algeria, in 1985, the M.S. degree in electrical engineering in 1989. and the Ph.D. degree in physics in 1994, both from Washington University, St. Louis, MO.

He is interested in numerical methods in electromagnetics, numerical analysis, applied mathematics, applied physics, and application of quantum field theory in quantum many-particle systems.

Jens Bornemann (M'87–SM'90) was born in Hamburg, Germany, on May 26, 1952. He received the Dipl.-Ing. and the Dr.-Ing. degrees, both in electrical engineering, from the University of Bremen, Bremen, Germany, in 1980 and 1984, respectively.

From 1980 to 1983, he was a Research and Teaching Assistant in the Department of Microwave, University of Bremen, where he worked on quasiplanar configurations and computer-aided design of E-plane filter design. In 1985, after a two-year period as a consulting engineer, he joined the University of Bremen as an Assistant Professor. Since April 1988, he has been with the University of Victoria, Victoria, B.C., Canada, where he is currently a Professor in the Department of Electrical and Computer Engineering. His research activities include microwave/millimeter-wave components and systems design and problems of electromagnetic field theory in integrated circuits and radiating structures. He is a coauthor of *Waveguide Components for Antenna Feed Systems. Theory and Design* (Dedham, MA: Artech House, 1993) and has authored/coauthored more than 100 technical papers. He is a Registered Professional Engineer in the Province of British Columbia, Canada.

Dr. Bornemann was one of the recipients of the A.F. Bulgin Premium of the Institution of Electronic and Radio Engineers in 1983, and he has been a Fellow of the British Columbia Advanced Systems Institute, 1992–1995. He serves on the editorial board of the IEEE TRANSACTIONS ON MICROWAVE THEORY AND TECHNIQUES and the *International Journal of Numerical Modeling*.

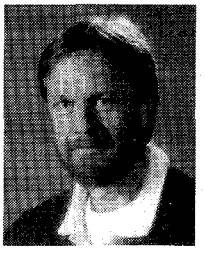

Ruediger Vahldieck (M'85–SM'86) received the Dipl.-Ing. and the Dr.-Ing. degrees in electrical engineering from the University of Bremen, Bremen, Germany, in 1980 and 1983, respectively.

From 1984 to 1986, he was a Research Associate at the University of Ottawa, Ottawa, Ont., Canada. In 1986, he joined the Department of Electrical and Computer Engineering at the University of Victoria, Victoria, B.C., Canada. Since 1991, he has been a Full Professor. During Fall and Spring 1992–1993, he was a Visiting Scientist at the "Ferdinand-Braun-Institute für Hochfrequenztechnik" in Berlin, Germany. His research interests include numerical methods to model electromagnetic fields for computer-aided design of microwave, millimeter-wave, and opto-electronic integrated circuits. In particular he is interested in design aspects of passive and active planar components for MIC and MMIC applications, as well as the development of CAD tools for filter structures, multiplexers, and polarizers. Recently, he became also involved in the design and simulation of broad-band fiber-optic communication systems and subsystems. He has published more than 100 technical papers, mainly in the field of microwave CAD.

Dr. Vahldieck, together with three coauthors, received the outstanding publication award of the Institution of Electronic and Radio Engineers in 1983. He is on the editorial board of the IEEE TRANSACTIONS ON MICROWAVE THEORY AND TECHNIQUES and he has served on the Technical Program Committee of the IEEE International Microwave Symposium since 1992.